Molecular Systems Biology 5; Article number 338; doi:10.1038/msb.2009.95
Citation: *Molecular Systems Biology* 5:338

www.molecularsystemsbiology.com

molecular systems biology

Chemogenomic profiling predicts antifungal synergies

Gregor Jansen[1,7,*], Anna Y Lee[2,3,7], Elias Epp[4,5], Amélie Fredette[1], Jamie Surprenant[1], Doreen Harcus[4], Michelle Scott[2,8], Elaine Tan[1], Tamiko Nishimura[1], Malcolm Whiteway[4,5], Michael Hallett[2,3,6] and David Y Thomas[1]

[1] Department of Biochemistry, Faculty of Medicine, McGill University, Montréal, Québec, Canada, [2] McGill Centre for Bioinformatics, McGill University, Montréal, Québec, Canada, [3] School of Computer Science, McGill University, Montréal, Québec, Canada, [4] Genetics Group, Biotechnology Research Institute, National Research Council of Canada, Montréal, Québec, Canada, [5] Department of Biology, McGill University, Montréal, Québec, Canada and [6] Rosalind and Morris Goodman Cancer Centre, McGill University, Montréal, Québec, Canada
[7] These authors contributed equally to this work
[8] Present address: School of Life Sciences Research, University of Dundee, Scotland DD1 5EH, UK
* Corresponding author. Department of Biochemistry, Faculty of Medicine, McGill University, McIntyre Medical Sciences Building, 3655 Promenade Sir William Osler, Montréal, Québec, Canada H3G 1Y6. Tel.: +1 514 398 1341; Fax: +1 514 398 7384; E-mail: gregor.jansen@mcgill.ca

Received 8.1.09; accepted 28.10.09

Chemotherapies, HIV infections, and treatments to block organ transplant rejection are creating a population of immunocompromised individuals at serious risk of systemic fungal infections. Since single-agent therapies are susceptible to failure due to either inherent or acquired resistance, alternative therapeutic approaches such as multi-agent therapies are needed. We have developed a bioinformatics-driven approach that efficiently predicts compound synergy for such combinatorial therapies. The approach uses chemogenomic profiles in order to identify compound profiles that have a statistically significant degree of similarity to a fluconazole profile. The compounds identified were then experimentally verified to be synergistic with fluconazole and with each other, in both *Saccharomyces cerevisiae* and the fungal pathogen *Candida albicans*. Our method is therefore capable of accurately predicting compound synergy to aid the development of combinatorial antifungal therapies.
Molecular Systems Biology **5**: 338; published online 22 December 2009; doi:10.1038/msb.2009.95
Subject Categories: functional genomics; computational methods
Keywords: antifungal; chemical genomics; drug profiling; synergy predictor

Introduction

Drugs that act against individual molecular targets are often insufficient to combat fungal infections, multigenic diseases such as cancer, and multiple cell or tissue type diseases, including immune and inflammatory disorders (White *et al*, 1998; Sams-Dodd, 2005; Onyewu and Heitman, 2007; Zimmermann *et al*, 2007). Combinatorial therapies that impact multiple targets simultaneously are less prone to development of drug resistance, and increase therapeutic efficacy (Groll and Walsh, 2002; Zimmermann *et al*, 2007). One of the major benefits of combinatorial therapies is the potential for synergistic effects: that is, the overall therapeutic benefit of the drug combination is greater than the sum of the effects of the individual agents. In particular, synergies between the constituent compounds can provide broader pharmacological windows and reduced toxicity (Fitzgerald *et al*, 2006). These advantages have driven drug discovery efforts towards the search for multi-agent therapies (Borisy *et al*, 2003; Fitzgerald *et al*, 2006; Onyewu and Heitman, 2007; Zimmermann *et al*, 2007).

Despite the obvious benefits, there are many challenges associated with the identification of multi-agent therapies. A sensitive, but low-throughput test for synergy is the dose-matrix response assay; in its simplest form it tests serial dilutions of two compounds in all possible permutations. The results from this assay can be analysed with respect to different models for quantifying synergy. Each model defines a baseline efficacy level for the compounds, when used in combination at concentrations X and Y, describing the expected level if the compounds are not synergistic. The Loewe additivity model defines the baseline as the level that would be expected if a compound were in fact combined with itself (Loewe, 1953). The Bliss boosting model, an extension of the Bliss independence model (Bliss, 1939), defines the baseline level as $I_{\mathrm{Mult}}=I_X+I_Y-I_XI_Y$, where I_X and I_Y are the efficacy levels of the compounds in isolation at concentrations X and Y, respectively (Lehár *et al*, 2007). Alternatively, the potentiation model defines the baseline level as $I_{\mathrm{Pot}}=\max(I_X, I_Y)$ (Lehár *et al*, 2007). The utility of any of these models depends on the comprehensiveness of the dose-matrix response data.

Large-scale searches have demonstrated that high-throughput screens of thousands of compounds can be straightforward (Zhang *et al*, 2007), but usually these screens can only test a small fraction of the exponential number of chemical

combinations available. Moreover, simplified dose-matrix assays are commonly used by these approaches, but the simplification may result in a failure to test the compound concentrations at which synergies occur, and therefore result in reduced synergy detection. Several lines of research address these problems (Borisy *et al*, 2003; Zhang *et al*, 2007). Some efforts reduce the scale issue by screening only combinations that include a particular compound of interest (i.e. by fixing one component). Other approaches tackle challenges later in the therapy development pipeline using *in silico* approaches to predict how two compounds act on pathways to achieve additive or synergistic effects (Lehár *et al*, 2007).

Although improvements in the scale and sensitivity of synergy identification techniques promise a greater exploration of combinatorial chemical space, it is unlikely that experimental techniques will be sufficient to completely survey this vast space in a cost-effective and timely manner. Consequently, there is a clear need for an approach that winnows this space to a manageably large set of combinations that is enriched for synergistic combinations. The combinations in the set could then be rigorously tested experimentally. A suggested experimental approach to finding this set entails an iterative 'maximal damage' search (Ágoston *et al*, 2005; Lehár *et al*, 2008a). In each iteration of the search, the most effective combination from the previous iteration is tested with all other compounds separately to identify a combination that is more effective. However, this directed strategy starts with the most effective compound and will thus miss potentiating synergies between compounds that incur minimal damage separately. In contrast, an accurate *in silico* approach would alleviate this challenge of synergy identification by enabling comprehensive and efficient exploration of the combinatorial space. Such a strategy could employ data from single compound treatments to effectively predict which combinations are most likely to behave synergistically. There are several approaches in the literature, including that of Nelander *et al* (2008), that attempt to use data from perturbation screens and prior knowledge regarding the targets of compounds to model the effects of these compounds when they are used alone or in combination. This approach is currently limited to compounds with known targets, but such an approach could potentially be extended to predict synergistic compound pairs (Nelander *et al*, 2008).

The use of chemogenomic profiles offers promise for characterizing the global cellular response to an arbitrary compound, for predicting the mode of action of a compound, and for inferring the function of genes. Here we focus on chemogenomic profiles generated for *Saccharomyces cerevisiae* where each member of the yeast gene deletion library is grown in the presence of a particular compound, and the resultant growth fitness is recorded. Strains with reduced fitness in comparison with untreated or wild-type cells suggest that the loss of particular genes confers sensitivity to the compound. For example, a set of genes involved in multi-drug resistance was identified by finding commonalities between yeast chemogenomic profiles of a chemically diverse panel of compounds (Parsons *et al*, 2004; Hillenmeyer *et al*, 2008). It has also been established that similarity between chemogenomic profiles often implies a similarity in the mode of action of the corresponding compounds (Parsons *et al*, 2006). In other words, two compounds that induce sensitivity in many of the same gene deletion strains may target similar cellular pathways. Conversely, strains that behave similarly across a panel of compounds may indicate that the corresponding genes are functionally related (Haggarty *et al*, 2003; Lee *et al*, 2005; Brown *et al*, 2006). The ability of chemogenomic profiles to predict similarities in cellular response, mode of action, and gene function poses the question as to whether they can be used to also predict synergy. This aspect has not been investigated to date and would provide a simple approach to synergy prediction that does not require prior knowledge of the targets of compounds and extensive modelling of previous approaches (Nelander *et al*, 2008).

We introduce here a combined experimental and bioinformatics approach to identify antifungal synergies. In particular, for each compound of interest, we obtain a chemogenomic profile, which we define as a set of genes whose deletions confer sensitivity to a given compound. The next step is to computationally measure the similarity between pairs of profiles. We establish that compound pairs that have correspondingly similar profiles are more likely to be synergistic when compared with randomly chosen compounds. This approach exploits the fact that chemogenomic profiles make compounds instantly comparable *in silico*: whereas exhaustive screening of only pairwise combinations already necessitates a quadratic number of dose-matrix assays, the computational method requires only a linear number of chemogenomic profiles and a small number of subsequent validation assays relative to the total number of possible combinations. Our approach is thus a practical way to comprehensively search the vast chemical space for synergistic compounds.

We validate this method by assessing the antifungal activity of compound combinations in *S. cerevisiae* and in the fungal pathogen *Candida albicans*. Infections by *Candida species* are an increasing problem, especially in patients who are immunocompromised (Groll and Walsh, 2002). We show that our approach successfully predicts antifungal synergies that occur in *S. cerevisiae* and *C. albicans*.

Results

Our goal was the identification of compound pairs that exhibit antifungal synergy. There are two types of antifungal synergy: the constituent compounds act synergistically to kill fungal cells (cytotoxic synergy) or arrest growth only (fungistatic synergy). Although a combination may be fungistatic against one fungal species, it might exhibit more potent synergy against others. Therefore, it may be useful to further investigate whether combinations that are fungistatic against particular fungal species can be developed into antifungal therapies against other fungal species.

The collection and generation of chemogenomic profiles

S. cerevisiae, with its accessible genetic resources, was used as the model for fungal pathogens. The first step in our method was to collect from the literature the results of ~1300

genome-wide, sensitivity and lethality screens generated with a broad range of compounds (Supplementary Table SI). This set forms our chemogenomic profile collection (Figure 1A). Although the screens were conducted differently (e.g. with diploids versus haploids; competitive versus non-competitive growth), the results of each screen permit the identification of a set of strains that are hypersensitive to the compound, which in turn define a set of hypersensitive genes. We focus on this hypersensitive gene set format of a chemogenomic profile in our analyses.

Fluconazole, a widely used fungistatic drug with favourable pharmacokinetic and toxicological properties (Grant and Clissold, 1990), would be an ideal constituent compound of a combinatorial antifungal therapy. We thus generated a *de novo* profile for fluconazole using the yeast haploid deletion strain collection (Winzeler *et al*, 1999). As a control, we used the hypomorphic strain for the essential gene *ERG11* (Schuldiner *et al*, 2005; Breslow *et al*, 2008). Fluconazole directly targets Erg11p and thus specifically inhibits its enzymatic activity in the biosynthetic pathway for ergosterol, an essential sterol in yeast (White *et al*, 1998). As expected, fluconazole was lethal to the *erg11* strain since inhibition of the already limited cellular amount of Erg11p likely decreased its activity to fatal levels. Although previous studies have identified strains that are sensitive to fluconazole (Parsons *et al*, 2004), we re-screened the drug to focus on deletions that are lethal in the presence of fluconazole. The results define a set of genes that we call FCZ-Fungicidal (Supplementary Table SII). We next validated the profile by determining the minimum inhibitory concentration (MIC) and minimum fungicidal concentration (MFC) for each strain (Figure 1B and Supplementary Table SIII). These values represent dosages where FCZ-Fungicidal strains are unable to recover after exposure to fluconazole, unlike wild-type cells.

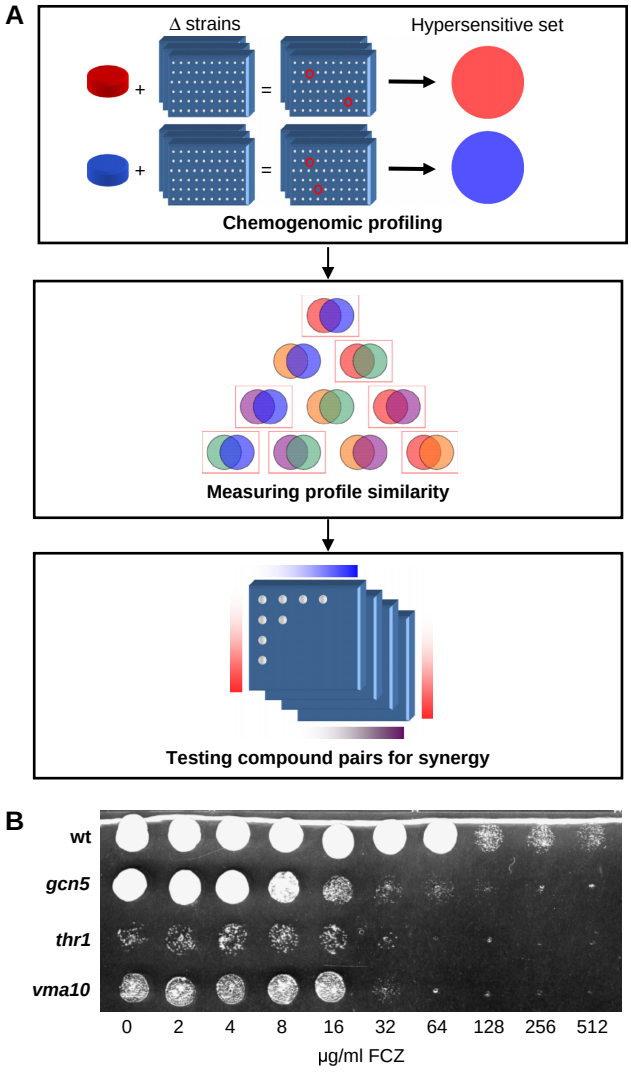

Figure 1 A method for identifying synergistic compounds with antifungal activity. (**A**) A schematic illustrating the steps of the method. (**B**) Validation of the first step: recovery after fluconazole treatment for defining the chemogenomic profile of the drug. Strains were treated with increasing amounts of fluconazole (0–128 μg/ml) for 24 h before spotting aliquots on YPD and incubating at 30°C for 2 days.

To exclude the possibility that any secondary mutations present in the deletion strains were responsible for the FCZ-Fungicidal phenotype, we complemented the FCZ-Fungicidal strains with plasmid-borne copies of their respective deleted genes to demonstrate reversibility of the phenotype. The presence of the overexpressed gene enabled the transformants to survive lethal concentrations of fluconazole above their MFCs (data not shown) without conferring resistance to fluconazole beyond levels observed for the wild type. Therefore, the complementation results confirm, for every FCZ-Fungicidal strain, that the gene deletion is responsible for the FCZ-Fungicidal phenotype.

Components of the FCZ-Fungicidal set

Of the 4997 deletion strains screened, 21 were unable to recover after exposure to fluconazole, in addition to the *erg11* hypomorphic strain (Supplementary Table SII). Members of the SAGA histone acetyltransferase complex and genes with general RNA polymerase-II transcription factor activity (e.g. members of the mediator complex) are significantly over-represented in the FCZ-Fungicidal set (adjusted $P=3.7\times10^{-6}$ and 0.01, respectively; see Materials and methods). Members of the vacuolar membrane H^+-ATPase complex and cytoskeleton genes are also over-represented in the set (adjusted $P=3.7\times10^{-6}$ and 0.03, respectively; see Materials and methods). Taken together, genes involved with transcriptional regulation, vacuole function, and cell structure are significantly associated with sensitivity to fluconazole.

Prediction of synergistic compounds

We assessed whether any given compound pair with a high level of similarity between its chemogenomic profiles is likely to exhibit antifungal synergy. A gold standard set of positive and negative examples of antifungal synergy was assembled for this purpose (Supplementary Table SIV). Specifically, the positive and negative examples are synergistic compound pairs curated from the literature and pairs that we showed are not synergistic in *S. cerevisiae* using a dose-matrix response assay (see Materials and methods; Supplementary Table SV), respectively. Moreover, the gold standard set is limited to

compound pairs where each constituent compound is associated with at least one chemogenomic profile in our collection. Although it would be interesting to investigate the potential differences in the accuracy of a synergy predictor built exclusively from either diploid- or haploid-based profiles, there are too few gold standard examples that are associated with both types of profiles to enable such a comparison (i.e. four positive examples). Similarly, there are too few examples to compare the accuracy of predictors built exclusively from either profiles generated from competitive or non-competitive growth assays (the literature contains only one positive example). Therefore, the gold standard set, together with our complete chemogenomic profile collection, was used to evaluate three different pairwise measures of chemogenomic profile similarity for their ability to predict antifungal synergy.

Previous studies suggest that the vast majority of compound pairs do not exhibit antifungal synergy. For example, Borisy *et al* (2003) tested 560 reference-listed compounds (i.e. known to have some bioactivity) in pairwise combination with fluconazole using a dose-matrix proliferation assay using fluconazole-resistant *C. albicans*. They described one synergistic combination, although they also confirmed 20 combinations as potentially synergistic because each of these combinations shows an effect that is greater than the baseline level defined by the highest single-agent model, that is, the larger of the effects produced by the constituent agents when they are applied singly. Overall, their results suggest that 0.2–3.6% of the tested combinations exhibit antifungal synergy (and the limited number of antifungal synergies reported in the literature in general suggests that synergy is even rarer in other chemical libraries). The scarcity of synergy would suggest that the evaluation of a synergy predictor should place great emphasis on the identification of true synergies.

It is standard practice to evaluate a predictor by estimating its receiver-operating characteristic (ROC) curve. However, applying this type of evaluation to a synergy predictor would equally emphasize the identification of true synergies and false positives. Furthermore, the estimated rarity of antifungal synergy implies that a ROC curve would be estimated with a very small fraction of all negative examples of synergy in the chemical space covered by our chemogenomic profile collection. That is, only 30 out of the estimated ~175 000 negative examples are known in our study, where the total number of negative examples is based on the estimated frequency of antifungal synergy, 3.6% (Borisy *et al*, 2003). A ROC curve estimated with the small negative gold standard set would likely hide the utility of the synergy predictor simply because our sample of negative examples is not sufficiently representative of the complete negative set. Therefore, instead of estimating ROC curves, we evaluated each synergy predictor by estimating to what degree its predictions are enriched for true synergies. That is, we computed a prediction score for every positive and negative example in our gold standard set and estimated to what degree the subset predicted to be synergistic is enriched with positive examples (with a hypergeometric test). This type of evaluation places greater value on the identification of true synergies as desired. We also estimated the true synergy enrichment of predictions made using random permutations of our chemogenomic profile collection (see Materials and methods). The enrichment estimates from the permutations establish a baseline enrichment distribution. The significance of the true synergy enrichment from the observed data was computed relative to this baseline distribution. Significant enrichment would suggest that testing a set of compound pairs that are predicted to be synergistic via profile similarity is expected to yield significantly more true synergies than testing an equal number of randomly selected compound pairs.

The first measure of chemogenomic profile similarity that we assessed quantifies the significance of the overlap between two hypersensitive gene sets (see the example in Figure 2A). In particular, when x genes are observed in both hypersensitive gene sets, the measure is the probability of obtaining x or more genes in the overlap by chance (i.e. a P-value from a hypergeometric distribution). With this gene-based profile similarity measure, a compound pair is predicted to be synergistic if its P-value is less than or equal to a given

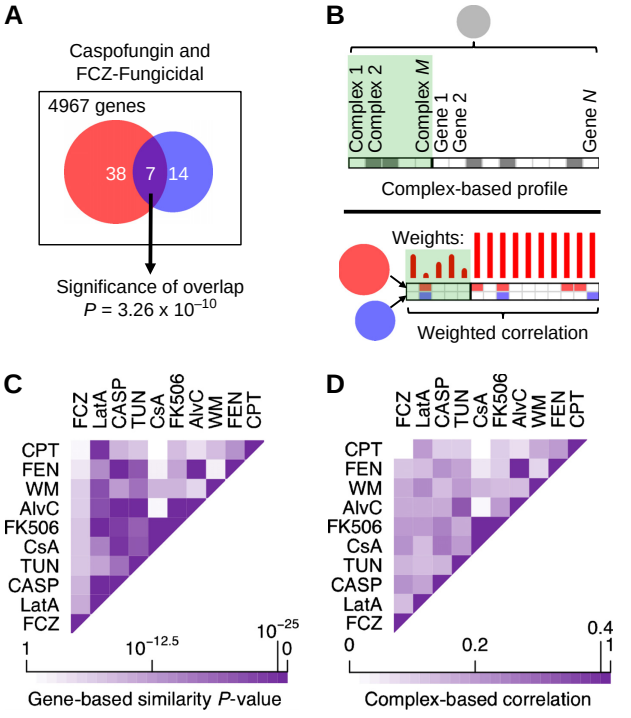

Figure 2 The measures of chemogenomic profile similarity and antifungal synergy predictions based on these measures. (**A**) An example of how the gene-based measure quantifies profile similarity with the hypergeometric test. (**B**) The complex-based measure. This measure compares complex-based profiles derived from hypersensitive gene sets. The similarity between the complex-based profiles is measured with weighted Pearson correlation. A protein complex is weighted less if it has many subunits, and all genes that are not annotated to any complex (i.e. non-complex genes) are assigned maximal weight. (**C**) A heatmap of the similarity values of select compound pairs, using the gene-based measure. The intensity of purple for a pair corresponds to the degree of similarity. All compounds in the heatmap are predicted as synergistic with fluconazole (using a threshold of $P \leqslant 10^{-6.5}$), except for camptothecin (included for contrast). (**D**) As in panel C, except that the similarity values were computed using the complex-based measure. AlvC, alverine citrate; CASP, caspofungin; CsA, cyclosporine-A; FCZ, fluconazole; FEN, fenpropimorph; LatA, latrunculin-A; TUN, tunicamycin; WM, wortmannin.

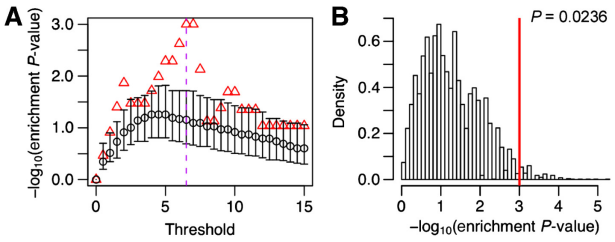

Figure 3 Statistical evaluation of the gene-based chemogenomic profile similarity measure as a predictor of antifungal synergy. The evaluation is based on the enrichment of the predictions with true positives/synergies, and higher values in this figure indicate greater enrichment. Baseline enrichment values were estimated using random permutations of the data (n=5000 permutations, see Materials and methods). The significance of the enrichment estimated from the observed data is computed relative to the baseline enrichment values. (**A**) The true synergy enrichment estimated from observed and randomly permuted data, at different similarity thresholds. The x-axis shows the $-\log_{10}$ transformation of the threshold values. The triangles indicate the enrichment values estimated from the observed data, at different thresholds. For each threshold, the median (o) and interquartile range (whiskers) of the enrichment values computed from the different permutations are also shown. (**B**) The significance of the true synergy enrichment associated with the predictor used with a threshold of $10^{-6.5}$, relative to the permutation distribution of the baseline enrichment. The red line indicates the enrichment estimated from the observed data and its P-value of significance is also shown. The threshold of $10^{-6.5}$ results in the most significant enrichment and is therefore considered the optimal profile similarity threshold for defining the synergy predictions.

threshold. We evaluated this profile similarity measure as a synergy predictor at different thresholds (Figure 3A). The predictions defined by the threshold $P \leqslant 10^{-6.5}$ exhibit a true synergy enrichment that represents a significant improvement over the expected baseline level (P=0.0236; see Figure 3B). Furthermore, this threshold produces the most significant improvement and is thus optimal for defining synergy predictions. Taken together, these results suggest that chemogenomic profile similarity predicts antifungal synergy.

We also assessed a chemogenomic profile similarity measure that accounts for additional commonality that is observable by viewing the profiles at the level of protein complexes (Figure 2B). That is, although one subunit of a protein complex may be associated with sensitivity to one compound and a different subunit associated with a second compound, it is nonetheless interesting that the same complex is associated with sensitivity to either compound. Each profile was converted into a complex-based profile defined by a list of 0 s and 1 s indicating absence or presence (respectively) of each complex, and also each non-complex gene, in the hypersensitive gene set. The similarity between two such profiles was measured via weighted Pearson correlation. A protein complex with many subunits is weighted less because it is less rare for that complex, via any one of its subunits, to be included in any given hypersensitive gene set. As with the gene-based profile similarity measure, a compound pair is predicted to be synergistic if the similarity of the corresponding profiles is greater than or equal to an optimal threshold. The enrichment of the predictions with true synergies is more significant for the complex-based measure than for the gene-based measure, relative to the expected baseline levels (P=0.0092 and 0.0378, respectively; see Supplementary Figure S1A). Taken together, these results suggest that the complex-based profile similarity measure can predict synergy more effectively than the simpler gene-based measure.

Lastly, we assessed a profile similarity measure that exploits the detailed quantitative data available for a subset of our chemogenomic profile collection. Namely, for some profiles each gene is associated with a $\log_2$ratio that reflects the growth of untreated versus chemically treated cells of the relevant deletion strain (Parsons *et al*, 2006; Hillenmeyer *et al*, 2008; Hoon *et al*, 2008). We thus considered the correlation across these $\log_2$ratios as a measure of profile similarity. Again, a compound pair is predicted to be synergistic if the similarity of the corresponding profiles is greater than or equal to an optimal threshold. Unlike measures of profile similarity based on hypersensitive gene sets, enrichment of the predictions with true synergies is not significant for the $\log_2$ratio-based measure, relative to the expected baseline level (P=0.3109; see Supplementary Figure S1A). Therefore, we focus on the gene-based profile similarity measure as a predictor of synergy (using the threshold $P \leqslant 10^{-6.5}$) due to its simplicity and significant enrichment of its predictions with true synergies (Figure 1A).

Consistent with the evidence that antifungal synergy is rare, the majority of compound pairs in the chemical space covered by our chemogenomic profile collection are not predicted to be synergistic (see the x-axis of Supplementary Figure S2A). In addition, the estimated accuracy of the predictor (=0.745) is significantly above the expected baseline level (P=0.018; see Supplementary Figure S2B), despite the fact that the estimate is likely based on a small fraction of all negative examples. If instead we over-estimate and assume that all compound pairs in our chemical space are negative examples (i.e. ∼182 000 instead of the estimated ∼175 000 examples, where the total number of negative examples is based on the estimated frequency of antifungal synergy, 3.6%; Borisy *et al*, 2003), our estimates would be based on a more representative set of negative examples (see Supplementary Figure S2A for the ROC curve). At the selected threshold, the estimated true positive rate is ∼67% and, using the overlarge negative set, the estimated false positive rate and accuracy are ∼5 and ∼95%, respectively. Furthermore, the level at which the predictions are enriched with true synergies would increase if the number of negative examples in the gold standard set were to increase and if all new examples were predicted as true negatives (Supplementary Figure S2C). Taken together, we have shown statistically that the predictor is surprisingly accurate and the estimate of its accuracy will increase as the community develops a more representative gold standard set. Therefore, we have shown that our predictor is useful for efficient identification of antifungal synergies.

The next step in the synergy identification method for our fluconazole example requires measuring the similarity between the FCZ-Fungicidal profile and each member of the chemogenomic profile collection. The FCZ-Fungicidal profile is significantly similar to 10 profiles ($P \leqslant 10^{-6.5}$) and these other profiles are associated with eight different compounds (Supplementary Table SVI). Consequently, eight compounds are predicted to be synergistic with fluconazole through the FCZ-Fungicidal profile.

Validation of predicted synergies in *S. cerevisiae*

Of the eight compounds predicted to be synergistic with fluconazole through the FCZ-Fungicidal profile, seven were tested for fungistatic and cytotoxic synergy with fluconazole in *S. cerevisiae*: latrunculin-A, caspofungin, tunicamycin, cyclosporine-A, FK506, alverine citrate, and wortmannin. Fenpropimorph is predicted to be synergistic with fluconazole through a different fluconazole profile (P=9.20 × 10^{-45}). Therefore, we also included fenpropimorph in our synergy tests. In total, eight predicted fluconazole combinations were experimentally tested for synergy.

We experimentally examined each compound combination using a dose-matrix response assay that measures the growth of treated cells. The results were used to quantify growth arrest synergy using the Loewe additivity model (Loewe, 1953; Barchiesi *et al*, 1998) (see Materials and methods; Supplementary Table SV). The dose-matrix response data were also fitted to Bliss boosting and potentiation models of synergy (Lehár *et al*, 2007) (see Materials and methods; Supplementary Table SVII). There is partial agreement between the results from the Loewe additivity model and the other models. However, we chose to identify synergies relative to the additive compound-with-itself baseline since it is the most conservative of the tested models. Each dose matrix of treated cells was also spotted on YPD to examine recovery of the cells post treatment (Figure 4). Absence of visible colonies after 24 h suggests that the treatment has some cytotoxic effects. Synergy in terms of this cytotoxic phenotype was also quantified with the Loewe additivity model (see Materials and methods). The cytotoxicity of compound combinations at particular concentrations was confirmed by a large reduction in the number of colony-forming units of treated versus untreated cells (data not shown). Compound combinations that exhibit growth arrest but not cytotoxic synergy are referred to as exhibiting fungistatic synergy. Figure 4C and D show examples of fungistatic and cytotoxic synergy (respectively) in *S. cerevisiae*.

Five compounds were validated as synergistic with fluconazole, including fenpropimorph (Supplementary Figure S3A and Table SV). Furthermore, we noticed that many of the compounds predicted to be synergistic with fluconazole are also predicted to be synergistic with each other (Figure 2C). The same observation can be made based on predictions with the complex-based profile similarity measure (Figure 2D). We thus extended our validation efforts to include 10 pairings of the predicted fluconazole partners. These pairings include two that are not predicted to be synergistic: cyclosporine-A + fenpropimorph and fenpropimorph + wortmannin. Of the 18 experimentally tested combinations in total, 11 showed a synergistic relationship with six and five demonstrated fungistatic and cytotoxic effects, respectively (Table I and Supplementary Figure S3 and Table SV). The two synergies involving fenpropimorph listed above are false negatives, although they are consistent with the observation that compounds that are synergistic with fluconazole tend to be synergistic with each other. Taken together, the results indicate a validation success rate of 56% in *S. cerevisiae*.

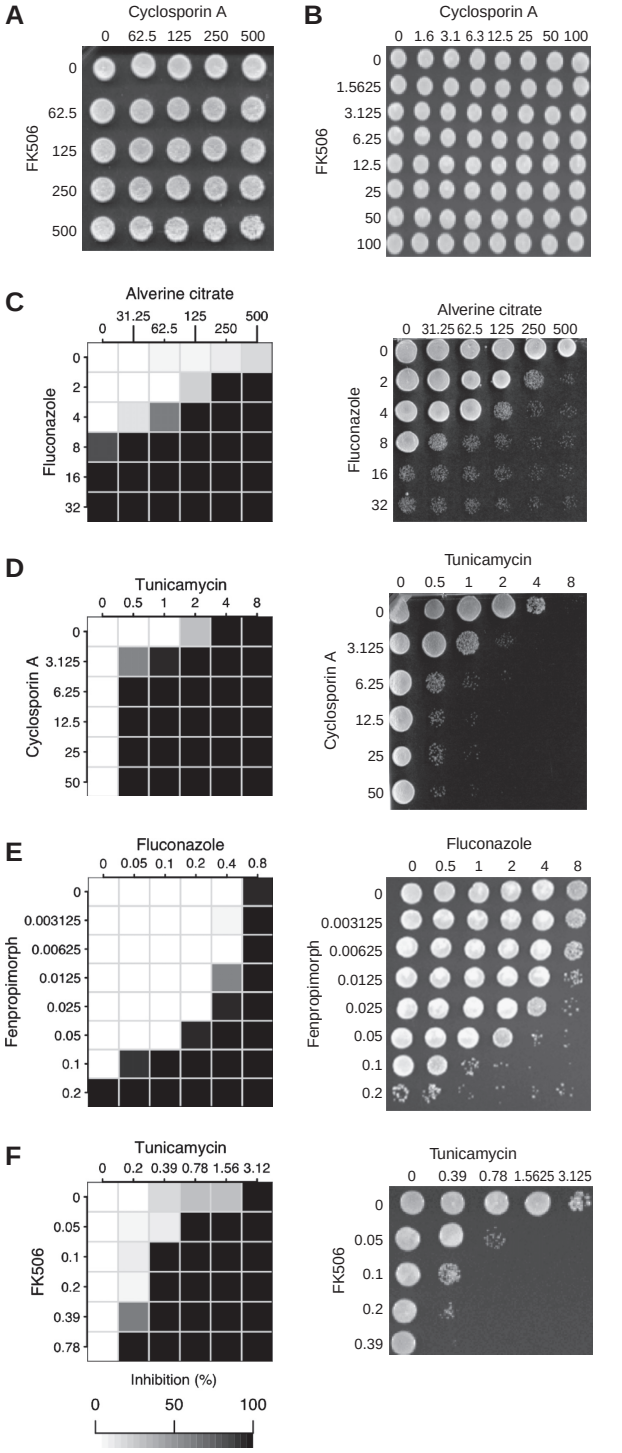

Figure 4 Dose-matrix responses to compound pairs that exhibit antifungal synergy. (C–F) Growth inhibition levels of cells grown in the presence of the compounds are shown on the left. The recovery of cells post treatment is shown on the right. (**A**, **B**) Recovery of cells treated with a compound pair that is not synergistic in *S. cerevisiae* and *C. albicans*, respectively. (**C**, **D**) Compound pairs that exhibit fungistatic and fungicidal synergy in *S. cerevisiae*, respectively. (**E**, **F**) Compound pairs that exhibit fungistatic and fungicidal synergy in *C. albicans*, respectively.

Validation of predicted synergies in *C. albicans*

We sought to identify synergies in *C. albicans* that establish potential multi-agent therapies, after validating our approach in the model *S. cerevisiae*. Four compound pairs that we identified as synergistic in *S. cerevisiae* are already described in the literature as synergistic in *Candida* species, suggesting that

our approach may successfully identify synergies in *C. albicans* (Table I). Using the dose-matrix response assay, the 18 combinations tested in *S. cerevisiae* were tested in *C. albicans* resulting in the identification of 10 synergistic combinations in the fungal pathogen, nine of which are cytotoxic (see Figure 4E and F for examples of fungistatic and cytotoxic synergy, respectively, and see Supplementary Figure S4 for all synergies identified in *C. albicans*). As before, we used the Loewe additivity model to quantify synergy (Supplementary Table SVIII), although we also fitted the dose-matrix response data to other synergy models (Supplementary Table SIX). Table I lists the complete set of synergistic compound pairs that we identified. We showed that eight synergistic combinations identified in *S. cerevisiae* are also synergistic in *C. albicans*, and we identified two additional synergies in the fungal pathogen that could not be identified in *S. cerevisiae* (caspofungin + fluconazole and fluconazole + latrunculin-A). Taken together, the validation success rate for the predictor of antifungal synergy is 69%. This implies that our method identifies true synergies at a rate that is ~20-fold better than the estimated rate for testing randomly selected compound pairs.

Table I Compound pairs that exhibit antifungal synergy

Compound pair	*S. cerevisiae*	*C. albicans*
AlvC + FCZ	Fungistatic	Cytotoxic
CASP + FCZ	—	Cytotoxic
CsA + FEN[a]	Fungistatic	Cytotoxic
CsA + FCZ[a]	Cytotoxic	Cytotoxic
CsA + TUN	Cytotoxic	Cytotoxic
FEN + FK506[a]	Fungistatic	—
FEN + FCZ	Fungistatic	Fungistatic
FEN + WM	Cytotoxic	—
FK506 + FCZ[a]	Fungistatic	Cytotoxic
FK506 + TUN	Cytotoxic	Cytotoxic
FK506 + WM	Cytotoxic	—
FCZ + LatA	—	Cytotoxic
FCZ + WM	Cytotoxic	Cytotoxic

AlvC, alverine citrate; CASP, caspofungin; CsA, cyclosporine-A; FCZ, fluconazole; FEN, fenpropimorph; LatA, latrunculin-A; TUN, tunicamycin; WM, wortmannin.
[a]Previously shown to be synergistic.

Finally, we tested one of the novel synergistic combinations in fluconazole-resistant clinical isolates of *C. albicans*. These strains acquired fluconazole resistance by mutations that either lead to upregulation of the target of fluconazole (*ERG11*, strain S2; Dunkel *et al*, 2008), or increased the expression of a multi-drug efflux pump (*MDR1*, strain G5; Morschhauser *et al*, 2007). We chose to test fluconazole (FDA-approved) in combination with wortmannin, analogues of which are in phase-I clinical trials (Noble *et al*, 2004). Even when applied at concentrations ~1000-fold higher than the MIC in corresponding wild-type strains, fluconazole has no readily detectable effect on cell growth in the clinical isolates. However, the combination of fluconazole and wortmannin exhibits a strong cytotoxic effect (Figure 5), suggesting potential clinical relevance.

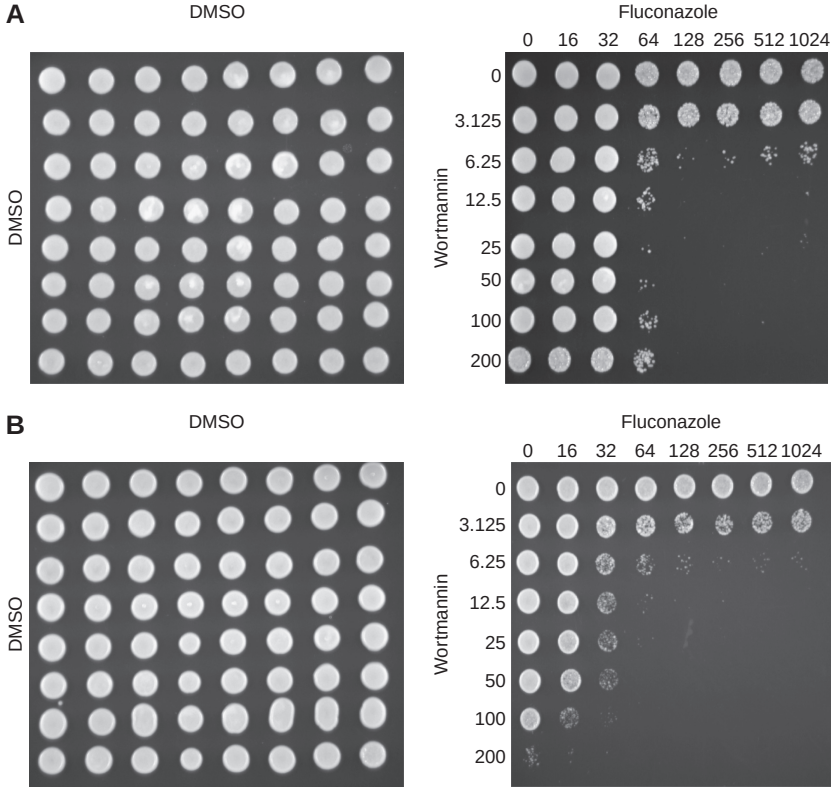

Figure 5 The dose-matrix recovery from treatment with fluconazole and wortmannin, a compound pair exhibiting antifungal synergy in (**A**) the multidrug-resistant clinical *C. albicans* isolate G5 and (**B**) the fluconazole-resistant clinical *C. albicans* isolate S2. Solvent controls are shown on the left.

A comparison of predictors dependent on haploid- and/or diploid-based profiles

After adding our novel synergistic compound pairs to the gold standard set of antifungal synergies, we revisited the question of whether the type of chemogenomic profiles used by the synergy predictor influences the enrichment of its predictions with true synergies. We therefore measured the significance of the enrichment associated with predictors dependent on haploid-based profiles only, diploid-based profiles only, and both haploid- and diploid-based profiles. However, this comparison could only be made using profiles generated from a competitive growth assay (i.e. the assay can use haploids or diploids) since there is an insufficient number of gold standard examples to also make the comparison in the context of profiles generated from a non-competitive growth assay. Although augmenting the gold standard set with validated synergies from this study may bias the enrichment values, all three predictors were subjected to the same bias since they were all evaluated with the same gold standard set, and here we are only interested in comparing the predictors relative to each other. As before, optimal prediction thresholds were selected for each of the three variants of the synergy predictor in the comparison. Our results suggest that the variant that exclusively uses haploid-based profiles produces predictions that are enriched with true synergies most significantly relative to the expected baseline enrichment level, followed by the variant that uses both haploid- and diploid-based profiles and the variant that exclusively uses diploid-based profiles (P=0.0372, 0.0572, and 0.0794, respectively; see Supplementary Figure S1B). However, our collection of haploid-based profiles contains data for only 20 compounds. Therefore, it is currently best to use all types of chemogenomic profiles with our approach for better coverage of chemical space, and thus, for enabling potential identification of more synergistic combinations.

Our results show that chemogenomic profile similarity predicts antifungal synergy. The similarity values for all pairings of the chemogenomic profiles in our collection are contained in Supplementary Table SX. These data can be used immediately to identify compound pairs that are likely to exhibit antifungal synergy, and thus should stimulate the search for effective combinatorial therapies.

Discussion

We have developed a bioinformatics-driven approach using chemogenomic profiles to predict compound pairs that exhibit antifungal synergy. First, we collected sensitivity-based chemogenomic profiles from the literature and generated a profile in *S. cerevisiae* for the widely used fungistatic drug fluconazole. We then showed statistical evidence supporting the use of our gene-based measure of profile similarity for predicting synergistic compound pairs. Our predictions of synergistic compound pairs validated with a high success rate. Overall, the results confirm that chemogenomic profile similarity can predict antifungal synergies.

Chemogenomic profiles can be generated in several ways. As more profiles of different type become available, it would be interesting to further investigate the relative utility of each type for the prediction of synergy. Our collection includes profiles based on competitive or non-competitive growth of diploids or haploids. Despite the heterogeneity of our collection, we used it in its entirety for better coverage of chemical space when predicting antifungal synergies. For example, had we limited the chemogenomic profile collection to haploid-based profiles, the cytotoxic synergy involving latrunculin-A would not have been predicted because a haploid-based profile was not generated for this compound. Despite the expected differences in the profiles simply due to the different ways in which they were generated, our approach was able to identify synergies based on the similarity between profiles generated with different methods (e.g. the FCZ-Fungicidal profile derived from non-competitive growth of haploids and the latrunculin-A profile derived from competitive growth of diploids). Therefore, different types of profiles may lead to false negatives; however, our approach generates predictions that are enriched with true antifungal synergies more significantly than what is expected by chance.

A chemogenomic profile encodes the genes involved in resistance to a particular compound (Lee *et al*, 2005; Parsons *et al*, 2006). If the profiles of two compounds are similar, there is likely some underlying drug-resistance machinery to which both apply stress. Cells treated with both compounds concurrently may not be able to mount an effective response to the challenge, and the compounds thus exhibit antifungal synergy. Previous studies have identified drug-resistance machinery (Parsons *et al*, 2004). Interestingly, the FCZ-Fungicidal set (Supplementary Table SII) includes the pleiotropic drug pump *PDR5*, genes that regulate the transcription of this pump as members of the SAGA and mediator complexes (Gao *et al*, 2004), and genes with vacuolar functionality. In short, the FCZ-Fungicidal set includes genes that have previously been associated with drug resistance. Our method, therefore, exploits the drug-response machinery identified by chemogenomic profiling to predict synergy.

The FCZ-Fungicidal set also includes genes associated with the cytoskeleton or cell wall, two of which (*BEM2*, *SLT2*) are synthetically lethal with the target of fluconazole, *ERG11* (Parsons *et al*, 2004). It is possible that these genes become vital for maintaining the structural integrity of the cell to compensate for the instability that may result from reduced ergosterol production. This is a possible explanation for why these genes are associated with resistance to fluconazole (i.e. if the genes are deleted, cells are hypersensitive to the drug). By similar reasoning, we would expect these genes to be associated with resistance to latrunculin-A, a compound that disrupts the actin cytoskeleton (Ayscough *et al*, 1997). Indeed, the hypersensitive gene set of latrunculin-A overlaps significantly with the FCZ-Fungicidal set, and the overlap includes genes associated with the cell wall or cytoskeleton (Supplementary Table SVI). Latrunculin-A was thus predicted as synergistic with fluconazole and this synergy was subsequently shown in *C. albicans*. Therefore, the FCZ-Fungicidal genes provide mechanisms to generate synergy.

Previous work suggests that compounds with similar chemogenomic profiles have similar modes of action (Parsons *et al*, 2004). However, in both *S. cerevisiae* and *C. albicans* we identified synergy between fluconazole and cyclosporine-A, which target ergosterol biosynthesis (White *et al*, 1998) and

calcineurin (Wang and Heitman, 2005), respectively. While fluconazole and cyclosporine-A profiles have distinguishing features (as expected due to the distinct targets of the compounds), our method uses a statistic that recognizes the profile similarities as significant, given what is possible by chance. That is, five genes in the overlap of the hypersensitive gene sets is in fact highly significant given that there are ~5000 possible genes for each set (with ~20 genes). As a predictor, our gene-based measure of profile similarity is thus useful for identifying synergies that might be unexpected given what is already known about the participating compounds.

The results establish that our method predicts synergy well in *S. cerevisiae*. It can also predict synergy in *C. albicans* based on chemogenomic profiles in *S. cerevisiae*. Despite differences in regulatory circuitry that have been observed between the fungal species (Martchenko *et al*, 2007; Hogues *et al*, 2008; Tuch *et al*, 2008), the majority of the synergies identified in *C. albicans* were transferred directly from *S. cerevisiae*. This suggests that the predicted synergies could be tested in *C. albicans* immediately, without first testing the predicted combinations in *S. cerevisiae* to filter out unlikely candidates. We have, therefore, shown that our method effectively uses *S. cerevisiae* resources to identify antifungal synergies in *C. albicans*. Furthermore, our method predicts synergies previously shown in other fungal pathogens (see Supplementary Table SIV for references) and it would thus be interesting to further investigate whether our method can predict broad-spectrum antifungal combinations that exhibit synergy.

We also statistically evaluated an alternative profile similarity measure, based on the correlation of $\log_2$ratios that quantify the growth of untreated versus treated cells, as a predictor of antifungal synergy. We found that this measure predicts synergy markedly worse than the validated gene-based measure (Supplementary Figure S1A). Interestingly, the gene-based measure compares $\log_2$ratio profiles by first converting them into hypersensitive gene sets. This suggests that the quantitative profile data that are useful for predicting synergy are effectively summarized by a hypersensitive gene set.

Our method for predicting antifungal synergy clearly requires chemogenomic profiles for compounds. Although construction of a chemogenomic profile for a compound is a significant task, the profile would be a beneficial resource in general because it is a multi-valued description of the bioactivity of a compound and can be used in all future studies. In fact, the number of published chemogenomic profiles is increasing (Lehár *et al*, 2008b) and as a result, the scope of our synergy prediction method is expanding.

Moreover, an alternative profile similarity measure was defined to enable analysis at the protein complex level. Statistical evaluation of this measure as a predictor of antifungal synergy (using the gold standard set) suggests that the measure actually predicts synergy better than the validated gene-based approach (Supplementary Figure S1A), although this may be an artefact of the small size of the gold standard set. Nevertheless, in combination with a variant of the complex-based measure, it may therefore be feasible to predict synergy using chemogenomic profiles built solely from strains pertaining to key members of protein complexes, thereby reducing the scale of the screening task. This would represent another important advance in our methodology.

In addition, our method is efficient because it is capable of reducing a huge set of all possible compound pairs down to a set of manageable size for thorough synergy testing in fungi and indeed may be applied to other organisms. Our results show that compounds that are synergistic with fluconazole tend to be synergistic with each other, suggesting that our method is also able to identify compound synergy clusters. Overall, the net gain from our method is greater compared with that from traditional screens since costs are reduced and sensitivity is increased.

Importantly, our method identified novel drug relationships, including cytotoxic synergy between fluconazole and wortmannin in *S. cerevisiae*, *C. albicans* and drug-resistant clinical isolates of *C. albicans*. Fluconazole is an FDA-approved drug and wortmannin analogues are in phase-I clinical trials (Noble *et al*, 2004). The method has thus uncovered a new synergistic combination that can be pursued as a viable therapy.

Combinatorial therapies have been widely used in different medical scenarios (Keith *et al*, 2005; Zimmermann *et al*, 2007). However, to discover new combinations using the vast number of compounds available (>10 million compounds available—http//www.emolecules.com), screening strategies must be adapted to address the scale of the discovery task. We have developed a powerful tool for rapid synergy discovery that represents a promising step towards realizing the potential of combinatorial therapies. We have validated this approach with antifungal combinations and pointed out a potential path to attack the persisting problem of drug-resistant *C. albicans* strains in the clinic. It would thus be interesting to investigate whether our approach can be used to streamline the combinatorial therapy development process in other therapeutic situations.

Materials and methods

Strains and media

The *S. cerevisiae* haploid strain BY4741 (*MAT**a**his3Δ1 leu2Δ0 met15Δ0 ura3Δ0*) and the complete yeast deletion array collection in the BY4741 background were obtained from the American Type Culture Collection. *S. cerevisiae* was cultured in rich media (YPD), synthetic complete media (SC), or synthetic drop-out media (SD-ura); for solid media 2% agar was added. The *C. albicans* wild-type strain SC5314, as well as the fluconazole- and multi-drug-resistant strains S2 (Dunkel *et al*, 2008) and G5 (Morschhauser *et al*, 2007), respectively, were cultured in YPDU media (YPD supplemented with 50 mg/l of uridine); for solid media 2% agar was added. Amiodarone, benomyl, camptothecin, carboplatin, fenpropimorph, FK506, fluconazole, mycophenolic acid, myriocin, tunicamycin, and wortmannin were dissolved in DMSO; chlorpromazine, desipramine, doxycycline, MMS, and nystatin were dissolved in water; and cyclosporine-A was dissolved in ethanol. Fluconazole was a gift from Pfizer Limited (Sandwich, Kent, UK), caspofungin was a gift from Merck Frosst Limited (Kirkland, Québec, Canada) and all other compounds were purchased from Sigma.

Library screen to generate the lethality-based chemogenomic profile for fluconazole

Ninety-six-well plates containing the American Type Culture Collection *S. cerevisiae* deletion strains were replicated with a 96-pin replicator (Boekel) to single-well Omnitray plates (Nalgene Nunc) containing YPD agar and geneticin (200 μg/ml), and, simultaneously, to plates containing YPD agar and fluconazole (85 μg/ml). The plates were incubated at 30°C for 48 h. Following incubation, cells on the YPD

control and fluconazole plates were replicated to fresh YPD plates (without fluconazole) and incubated at 30°C for 48 h. Plates were scored for deletion strains that were unable to grow after exposure to fluconazole. Strains that fit this criterion were subsequently retested in MIC and recovery assays (see below). The deletion strains that were unable to recover from fluconazole at concentrations that in contrast did not affect wild-type cells, were assigned a score of 1 in the chemogenomic profile and all other strains were assigned 0. Moreover, genes associated with the deletion strains with score 1 define our hypersensitive gene set for fluconazole (i.e. the FCZ-Fungicidal set).

MIC assays, recovery assays, and compound synergy tests in *S. cerevisiae* and *C. albicans*

Antifungal sensitivity testing was performed with a modified version of the CLSI (formerly NCCLS) procedure (NCCLS. Reference Method for Broth Antifungal Susceptibility Testing of Yeasts: Approved Standard-Second Edition. NCCLS document M27-A2). Briefly, overnight cultures of the wild-type and deletion strains were diluted to an OD_{600} of 0.0005 for *S. cerevisiae* and OD_{600} 0.001 for *C. albicans*. Volumes of 50 μl of culture were inoculated into 96-well flat-bottom plates containing 50 μl of SC media for *S. cerevisiae* and YPD media for *C. albicans* with increasing concentrations of compound (in twofold serial dilutions). The cultures were grown without shaking at 30°C for 24 h and OD_{600} measurements were taken with a Tecan Safire microplate monochromator reader (Tecan, Austria, GmbH). The MIC was determined by the first well with a growth reduction of at least 95% in the presence of a compound as compared with untreated cells. Cells were then spotted (2 μl) onto YPD plates and incubated at 30°C for 48 h to assess the extent to which cells recover from the treatments. The MFC of a given strain was determined from these recovery assays (Supplementary Tables SV and SVII).

Compound synergy interactions were assessed by growth in a dose-matrix titration assay. Volumes of 50 μl of each compound were twofold serially diluted in SC media for *S. cerevisiae* and YPD media for *C. albicans*, and dispensed into 96-well flat-bottom plates, either across columns of the plates (compound-A) or down rows of the plates (compound-B). Wells were then inoculated with 50 μl of wild-type yeast prepared as in the MIC assay. Plates were incubated at 30°C without shaking and OD_{600} measurements were taken after 24 h. MICs were determined for the compounds alone and in combination by the first well, with $\geqslant$95% decrease in absorbance relative to the control. The growth arrest synergy of a compound pair was quantified with respect to the Loewe additivity model (Loewe, 1953) through the fractional inhibitory concentration index $(FICI_{growthArrest}) = (MIC_{A\ in\ combo}/MIC_{A\ alone}) + (MIC_{B\ in\ combo}/MIC_{B\ alone})$. A compound pair is classified as synergistic if its FICI is $\leqslant$0.5, the standard threshold (Loewe, 1953; Barchiesi *et al*, 1998). Cells were also spotted (2 μl) onto fresh YPD plates and incubated at 30°C for 24 h to test for cytotoxic synergy. The minimum cytotoxic concentration (MCC) was defined for a compound alone and in combination as the lowest concentration that did not result in visible colonies on the plate. Cytotoxicity was confirmed by measuring colony-forming units (CFUs) after compound treatment. Cells were treated with both compounds at their MCCs, then plated on YPD plates and CFUs were counted after 48 h incubation at 30°C. The cytotoxic synergy of a compound pair was quantified as $FICI_{cytotoxic} = (MCC_{A\ in\ combo}/MCC_{A\ alone}) + (MCC_{B\ in\ combo}/MCC_{B\ alone})$. A compound pair was classified as exhibiting fungistatic synergy if we identified the pair as synergistic with respect to the growth arrest phenotype only.

Complementation assay

To demonstrate that fluconazole sensitivity was dependent on particular gene deletion and not on acquired secondary mutations, the deletion strains were transformed with plasmids carrying their respective deleted genes expressed from the galactose-inducible *GAL1* promoter (Gelperin *et al*, 2005; Jansen *et al*, 2005). The transformants were incubated in two sequential overnight cultures. Cells were diluted and treated with fluconazole as described above and then incubated at 30°C for 24 h. After incubation, 2 μl of cultures were spotted onto fresh YPD plates, incubated at 30°C for 2 days, and scored for growth. The complementation test was performed under both inducing (SC: 4% galactose) and non-inducing (SC: 2% glucose) conditions.

The chemogenomic profile collection

We collected the results of compound sensitivity screens described in the literature. Different screens used different schemes to score each deletion strain based on its observed level of sensitivity to a given compound (and the complete set of strain scores defines the chemogenomic profile of the compound). For each chemogenomic profile, we identified strains that were scored as moderately to highly sensitive to the compound by noting the strains with scores that surpass the threshold specified in Supplementary Table SI. The genes associated with these strains define the hypersensitive gene set of the compound.

Annotations of the FCZ-Fungicidal genes

Descriptions of the FCZ-Fungicidal genes were downloaded from the Saccharomyces Genome Database (SGD; ftp://ftp.yeastgenome.org/yeast/). Gene Ontology (GO)-based gene annotations (Ashburner *et al*, 2000) were used to test whether particular biological processes, molecular functions, and cellular components are significantly over-represented in the FCZ-Fungicidal gene set. For each GO gene set, a *P*-value was obtained from a hypogeometric test performed within the scope of the set of genes associated with strains that were used in the FCZ-Fungicidal screen. The *P*-values were adjusted for multiple comparisons using the Benjamini and Hochberg method (Benjamini and Hochberg, 1995).

The gold standard set

A gold standard set of positive and negative examples of antifungal synergy was assembled to evaluate the synergy predictors (Supplementary Table SIV). Specifically, the 21 positive examples are synergistic compound pairs curated from the literature. The 30 negative examples are pairs that we showed are not synergistic in *S. cerevisiae* using a dose-matrix response assay (Supplementary Table SV).

The measures of chemogenomic profile similarity

Consider profiles A and B and their associated hypersensitive gene sets G_A and G_B, respectively. Let U_A and U_B represent the sets of all genes associated with strains that were screened to generate profiles A and B, respectively. U_A and U_B may differ if, for example, one screen involved essential genes (through heterozygous strains) and the other did not. We define $U = U_A \cap U_B$ as the scope of the statistical test that measures the similarity between profiles A and B, and therefore compute $G_A' = G_A \cap U$ and $G_B' = G_B \cap U$.

The gene-based profile similarity measure compares the hypersensitive gene sets associated with the profiles. The measure is defined as the *P*-value obtained from a hypergeometric test that quantifies the significance of $|G_A' \cap G_B'|$ (i.e. the probability of obtaining an equal or larger number by chance), given $|G_A'|$, $|G_B'|$ and $|U|$.

The complex-based profile similarity measure compares hypersensitive gene sets that have been transformed into complex-based profiles (Figure 2B). Mappings of genes to GO-defined protein complexes were downloaded from SGD. Let C_i represent the set of genes associated with complex i. The GO hierarchy subdivides some complexes into its constituent domains. In these cases, we treat each domain as a separate complex, and the genes associated with the domains are removed from the gene set of the parent complex (to avoid redundancy). For protein complex i, we compute $C_i' = C_i \cap U$. If $G' \cap C_i' \neq \varnothing$, we say that complex i is present in G', else it is absent. We generate a complex-based profile $\mathbf{x}_A$, defined as a vector of 0 s and 1s indicating absence or presence (respectively) of each complex, and also each non-complex gene, in G_A'. Similarly, $\mathbf{x}_B$ was generated with G_B'. The similarity between $\mathbf{x}_A$ and $\mathbf{x}_B$ is measured via weighted

Pearson correlation. Each non-complex gene is assigned a full weight of 1 and complex i is assigned a weight equal to $1/|C_i'|$. That is, a protein complex with many subunits is weighted less because it is less rare (and thus less significant) for that complex, via any one of its subunits, to be present in any given G'.

The $\log_2$ratio-based profile similarity measure compares profiles that have $\log_2$ratio sensitivity scores. The $\log_2$ratios quantify the growth of untreated cells versus treated cells. We define $\mathbf{y_A}$ as the vector of $\log_2$ratios of profile A, with one value specified for each gene in U. Similarly, we define $\mathbf{y_B}$ for profile B, retaining the same gene order that is used in $\mathbf{y}_A$. The similarity between $\mathbf{y_A}$ and $\mathbf{y_B}$ is measured with Pearson correlation.

Synergy prediction

Our chemogenomic profile collection may contain several different profiles associated with a single compound. For example, these profiles may have been generated with different assays and/or different concentrations of the compound. For compounds A and B, every profile for A is compared to every profile for B. The similarity value for the compound pair is defined as the best similarity value obtained from all the pairwise profile comparisons. For the gene-based profile similarity measure, the best is the lowest P-value. If the similarity value of a compound pair is less than or equal to some threshold, the pair is predicted to be synergistic. For the complex-based and $\log_2$ratio-based measures, the best similarity value is the highest correlation value. For these measures, a compound pair is predicted to be synergistic if its similarity value is greater than or equal to some threshold.

For the comparison of the three profile similarity measures as predictors of synergy (Supplementary Figure S1A), a reduced gold standard set was used to evaluate each predictor (16 and 24 positive and negative examples, respectively). Each compound pair in the reduced set is associated with $\log_2$ratio profiles since the $\log_2$ratio-based measure requires these types of profiles (see Supplementary information).

Similarly, for comparison of the gene-based measure predictors dependent on haploid-based profiles only, diploid-based profiles only, and both types of profiles (Supplementary Figure S1B), a different gold standard set was used to evaluate these predictors (10 and 16 positive and negative examples, respectively). Each compound pair in the set is associated with both haploid-based and diploid-based profiles, and all the profiles were generated from a competitive growth assay. To avoid an extremely small number of positive examples, the set includes synergies validated in this study (see Supplementary information). Even so, there is insufficient number of gold standard examples to also make the comparison in the context of profiles generated from a non-competitive growth assay.

We evaluated each variant of the synergy predictor based on the significance of enrichment of its predictions with true positives/synergies, relative to the expected baseline level (see section Permutation analysis below). The optimal profile similarity threshold for defining the predictions of each variant is therefore the threshold that results in the most significant enrichment.

Permutation analysis

The chemogenomic profile labels were permuted 5000 times in order to estimate the baseline levels of different statistics, for each variant of the synergy predictor. For each type of profile (the type of each profile is specified in Supplementary Table SI), the labels were randomly permuted among all profiles of that type. This preserves any systematic differences between profiles of different type. However, we excluded permutations where at least one profile label is assigned to a profile corresponding to the same compound. For example, this could potentially occur when there are multiple profiles generated with different concentrations of the same compound. Additional restrictions were applied, depending on the type of analysis. For comparison between the three profile similarity measures, permutations were only performed across $\log_2$ratio profiles. For comparison of predictors dependent on haploid-based profiles only, diploid-based profiles only, and both types of profiles, permutations were only performed across profiles generated from a competitive growth assay. In addition, permutations were performed only across haploid- and diploid-based profiles for predictors exclusively dependent on haploid- and diploid-based profiles, respectively.

With each permutation, synergy predictions were made using a given variant of the predictor at different thresholds. We computed a statistic quantifying the enrichment of the predictions (defined by the optimal threshold) with true synergies. That is, the P-value obtained from a hypergeometric test that equals the probability of obtaining an equal or larger number of positive examples predicted to be synergistic by chance, given the numbers of positive examples, negative examples, and predicted synergies in the given gold standard set. For the final predictor, the predictions were also used to compute the accuracy at the optimal threshold.

For each statistic z (e.g. the enrichment P-value), a permutation distribution of the baseline value was obtained by collecting the computed values from all 5000 permutations. Moreover, the significance of the value computed with the observed/real data (z_{obs}) relative to the expected baseline value was quantified as $P=(x+1)/(n+1)$, where x is the number of permutations with a z value better than or equal to z_{obs} and $n=5000$, the number of permutations in this case (Moore *et al*, 2009).

Fitting to other models of synergy

For each compound pair that was experimentally tested for synergy, Bliss boosting and potentiation models of synergy were fit to the dose-matrix response data (Lehár *et al*, 2007). First, the OD_{600} values were used to compute a corresponding matrix of % inhibition values (I) relative to untreated cells. Model fits to the inhibition data were then obtained as previously described (Lehár *et al*, 2007). The sum-of-squared fit errors $(SS)=\Sigma(I_{observed}-I_{fit})^2$ was computed for each model. The best fit model was defined as the first consistent model, with the Bliss boosting model considered before the potentiation model because it is less complex. We define consistent as $|SS-SS_{min}|<SS_{min}$, where SS_{min} is the minimum SS of the two models.

A Bliss boosting surface is defined by $I_{Bliss}=I_X+I_Y+(\beta-E_{min})[(I_XI_Y)/(E_XE_Y)]$, where I_{Bliss} is the Bliss boosting inhibition level when both compounds are used in combination, with the first and second compounds used at concentrations X and Y, respectively. I_X and I_Y are the inhibition levels when the first and second compounds are used alone at concentrations X and Y, respectively. E_X and E_Y are the maximum inhibition levels achievable by the first and second compounds, respectively, and $E_{min}=\min(E_X, E_Y)$; β is the fitted parameter and it represents the amount of boosting above $\max(E_X, E_Y)$. Reference values of β indicate cancelling, suppressive, masking, multiplicative, and saturating levels of Bliss boosting. The selected Bliss boosting level of a compound pair is defined as the first consistent level (in the order shown above), where consistent is defined as $|\Delta\beta-\Delta\beta_{min}|<\Delta\beta_{min}$, with $\Delta\beta=|\beta-\beta_{ref}|$ for some reference level β_{ref}, and β_{min} is the minimum $\Delta\beta$ across all reference levels.

A potentiation model surface is defined by $I_{Potent}=\max(I_X(C), I_Y)$, where $I_X(C)$ is the inhibition level when the potentiated compound is used alone, at a shifted concentration C. We have that $C=X[1+(Y/Y_{pot})^{|p|}]^{sign(p)}$, where Y_{pot} and p are fitted parameters, representing the concentration of the potentiated compound above which potentiation occurs and the potentiation slope, respectively (Lehár *et al*, 2007). $P=0$, $P>0$, and $P<0$ indicate no potentiation, synergy, and antagonism, respectively. For each compound pair, the inhibition matrix was fitted to this model twice: the first time assuming that the first compound is potentiated, and the second time assuming that the second compound is potentiated. Of the two fits, we report the one with the lower SS (Supplementary Tables SVII and SIX).

All computational analyses were performed in the R statistical software framework (R Development Core Team, 2007).

Supplementary information

Supplementary information is available at the *Molecular Systems Biology* website (www.nature.com/msb).

Acknowledgements

We thank Dr Robert Annan for comments and suggestions regarding the writing of the paper. We thank Dr Charles Boone for providing additional chemogenomic profile data that were generated by Parsons *et al* (2006). This is National Research Council of Canada publication NRC 495413. This work was supported by the Natural Sciences and Engineering Research Council of Canada, and the Canadian Institutes of Health Research (scholarship to AYL and grants to MW, MH, and DYT).

Conflict of interest

The authors declare that they have no conflict of interest.

References

Ágoston V, Csermely P, Pongor S (2005) Multiple weak hits confuse complex systems: a transcriptional regulatory network as an example. *Phys Rev E Stat Nonlin Soft Matter Phys* **71:** 051909

Ashburner M, Ball CA, Blake JA, Botstein D, Butler H, Cherry JM, Davis AP, Dolinski K, Dwight SS, Eppig JT, Harris MA, Hill DP, Issel-Tarver L, Kasarskis A, Lewis S, Matese JC, Richardson JE, Ringwald M, Rubin GM, Sherlock G (2000) Gene ontology: tool for the unification of biology. The Gene Ontology Consortium. *Nat Genet* **25:** 25–29

Ayscough KR, Stryker J, Pokala N, Sanders M, Crews P, Drubin DG (1997) High rates of actin filament turnover in budding yeast and roles for actin in establishment and maintenance of cell polarity revealed using the actin inhibitor latrunculin-A. *J Cell Biol* **137:** 399–416

Barchiesi F, Di Francesco LF, Compagnucci P, Arzeni D, Giacometti A, Scalise G (1998) *In-vitro* interaction of terbinafine with amphotericin B, fluconazole and itraconazole against clinical isolates of *Candida albicans*. *J Antimicrob Chemother* **41:** 59–65

Benjamini Y, Hochberg Y (1995) Controlling the false discovery rate: a practical and powerful approach to multiple testing. *J R Stat Soc B* **57:** 289–300

Bliss C (1939) The toxicity of poisons applied jointly. *Ann Appl Biol* **26:** 585–615

Borisy AA, Elliott PJ, Hurst NW, Lee MS, Lehar J, Price ER, Serbedzija G, Zimmermann GR, Foley MA, Stockwell BR, Keith CT (2003) Systematic discovery of multicomponent therapeutics. *Proc Natl Acad Sci USA* **100:** 7977–7982

Breslow DK, Cameron DM, Collins SR, Schuldiner M, Stewart-Ornstein J, Newman HW, Braun S, Madhani HD, Krogan NJ, Weissman JS (2008) A comprehensive strategy enabling high-resolution functional analysis of the yeast genome. *Nat Methods* **5:** 711–718

Brown JA, Sherlock G, Myers CL, Burrows NM, Deng C, Wu HI, McCann KE, Troyanskaya OG, Brown JM (2006) Global analysis of gene function in yeast by quantitative phenotypic profiling. *Mol Syst Biol* **2:** 2006 0001

Cowen LE, Nantel A, Whiteway MS, Thomas DY, Tessier DC, Kohn LM, Anderson JB (2002) Population genomics of drug resistance in *Candida albicans*. *Proc Natl Acad Sci USA* **99:** 9284–9289

Dunkel N, Liu TT, Barker KS, Homayouni R, Morschhauser J, Rogers PD (2008) A gain-of-function mutation in the transcription factor Upc2p causes upregulation of ergosterol biosynthesis genes and increased fluconazole resistance in a clinical *Candida albicans* isolate. *Eukaryot Cell* **7:** 1180–1190

Fitzgerald JB, Schoeberl B, Nielsen UB, Sorger PK (2006) Systems biology and combination therapy in the quest for clinical efficacy. *Nat Chem Biol* **2:** 458–466

Gao C, Wang L, Milgrom E, Shen WCW (2004) On the mechanism of constitutive Pdr1 activator-mediated PDR5 transcription in *Saccharomyces cerevisiae*: evidence for enhanced recruitment of coactivators and altered nucleosome structures. *J Biol Chem* **279:** 42677–42686

Gelperin DM, White MA, Wilkinson ML, Kon Y, Kung LA, Wise KJ, Lopez-Hoyo N, Jiang L, Piccirillo S, Yu H, Gerstein M, Dumont ME, Phizicky EM, Snyder M, Grayhack EJ (2005) Biochemical and genetic analysis of the yeast proteome with a movable ORF collection. *Genes Dev* **19:** 2816–2826

Grant SM, Clissold SP (1990) Fluconazole. A review of its pharmacodynamic and pharmacokinetic properties, and therapeutic potential in superficial and systemic mycoses. *Drugs* **39:** 877–916

Groll AH, Walsh TJ (2002) Antifungal chemotherapy: advances and perspectives. *Swiss Med Wkly* **132:** 303–311

Haggarty SJ, Clemons PA, Schrieber SL (2003) Chemical genomic profiling of biological networks using graph theory and combinations of small molecule perturbations. *J Am Chem Soc* **125:** 10543–10545

Hillenmeyer ME, Fung E, Wildenhain J, Pierce SE, Hoon S, Lee W, Proctor M, St Onge RP, Tyers M, Koller D, Altman RB, Davis RW, Nislow C, Giaever G (2008) The chemical genomic portrait of yeast: uncovering a phenotype for all genes. *Science* **320:** 362–365

Hogues H, Lavoie H, Sellam A, Mangos M, Roemer T, Purisima E, Nantel A, Whiteway M (2008) Transcription factor substitution during the evolution of fungal ribosome regulation. *Mol Cell* **29:** 552–562

Hoon S, Smith AM, Wallace IM, Suresh S, Miranda M, Fung E, Proctor M, Shokat KM, Zhang C, Davis RW, Giaever G, St Onge RP, Nislow C (2008) An integrated platform of genomic assays reveals small-molecule bioactivities. *Nat Chem Biol* **4:** 498–506

Jansen G, Wu C, Schade B, Thomas DY, Whiteway M (2005) Drag&Drop cloning in yeast. *Gene* **344:** 43–51

Keith CT, Borisy AA, Stockwell BR (2005) Multicomponent therapeutics for networked systems. *Nat Rev Drug Discov* **4:** 71–78

Lee W, St Onge RP, Proctor M, Flaherty P, Jordan MI, Arkin AP, Davis RW, Nislow C, Giaever G (2005) Genome-wide requirements for resistance to functionally distinct DNA-damaging agents. *PLoS Genet* **1:** e24

Lehár J, Krueger A, Zimmermann G, Borisy A (2008a) High-order combination effects and biological robustness. *Mol Syst Biol* **4:** 215

Lehár J, Stockwell BR, Giaever G, Nislow C (2008b) Combination chemical genetics. *Nat Chem Biol* **4:** 674–681

Lehár J, Zimmermann GR, Krueger AS, Molnar RA, Ledell JT, Heilbut AM, Short III GF, Giusti LC, Nolan GP, Magid OA, Lee MS, Borisy AA, Stockwell BR, Keith CT (2007) Chemical combination effects predict connectivity in biological systems. *Mol Syst Biol* **3:** 80

Loewe S (1953) The problem of synergism and antagonism of combined drugs. *Arzneimittelforschung* **3:** 285–290

Martchenko M, Levitin A, Hogues H, Nantel A, Whiteway M (2007) Transcriptional rewiring of fungal galactose-metabolism circuitry. *Curr Biol* **17:** 1007–1013

Moore D, McCabe G, Craig B (2009) Bootstrap methods and permutation tests. In *Introduction to the Practise of Statistics*, Burke S, Scanlan-Rohrer A, Byrd M (eds), Vol. 16, 6th edn, pp 11–60. New York: WH Freeman and Company

Morschhauser J, Barker KS, Liu TT, Bla BWJ, Homayouni R, Rogers PD (2007) The transcription factor Mrr1p controls expression of the MDR1 efflux pump and mediates multidrug resistance in *Candida albicans*. *PLoS Pathog* **3:** e164

Nelander S, Wang W, Nilsson B, She QB, Pratilas C, Rosen N, Gennemark P, Sander C (2008) Models from experiments: combinatorial drug perturbations of cancer cells. *Mol Syst Biol* **4:** 216

Noble ME, Endicott JA, Johnson LN (2004) Protein kinase inhibitors: insights into drug design from structure. *Science* **303:** 1800–1805

Onyewu C, Heitman J (2007) Unique applications of novel antifungal drug combinations. *Anti-Infect Agents Med Chem* **6:** 3–15

Parsons AB, Brost ReL, Ding H, Li Z, Zhang C, Sheikh B, Brown GW, Kane PM, Hughes TR, Boone C (2004) Integration of chemical-genetic and genetic interaction data links bioactive compounds to cellular target pathways. *Nat Biotechnol* **22:** 62–69

Parsons AB, Lopez A, Givoni IE, Williams DE, Gray CA, Porter J, Chua G, Sopko R, Brost RL, Ho C-H, Wang J, Ketela T, Brenner C, Brill JA, Fernandez GE, Lorenz TC, Payne GS, Ishihara S, Ohya Y, Andrews B *et al* (2006) Exploring the mode-of-action of bioactive compounds by chemical-genetic profiling in yeast. *Cell* **126:** 611–625

R Development Core Team (2007) *R: a Language and Environment for Statistical Computing*. Vienna, Austria: R Foundation for Statistical Computing. ISBN 3-9000051-07-0, URL www.R-project.org

Sams-Dodd F (2005) Target-based drug discovery: is something wrong? *Drug Discov Today* **10:** 139–147

Schuldiner M, Collins SR, Thompson NJ, Denic V, Bhamidipati A, Punna T, Ihmels J, Andrews B, Boone C, Greenblatt JF, Weissman JS, Krogan NJ (2005) Exploration of the function and organization of the yeast early secretory pathway through an epistatic miniarray profile. *Cell* **123:** 507–519

Tuch BB, Galgoczy DJ, Hernday AD, Li H, Johnson AD (2008) The evolution of combinatorial gene regulation in fungi. *PLoS Biol* **6:** e38

Wang P, Heitman J (2005) The cyclophilins. *Genome Biol* **6:** 226

White TC, Marr KA, Bowden RA (1998) Clinical, cellular, and molecular factors that contribute to antifungal drug resistance. *Clin Microbiol Rev* **11:** 382–402

Winzeler EA, Shoemaker DD, Astromoff A, Liang H, Anderson K, Andre B, Bangham R, Benito R, Boeke JD, Bussey H, Chu AM, Connelly C, Davis K, Dietrich F, Dow SW, Bakkoury ME, Foury F, Friend SH, Gentalen E, Giaever G *et al* (1999) Functional characterization of the *S. cerevisiae* genome by gene deletion and parallel analysis. *Science* **285:** 901–906

Zhang L, Yan K, Zhang Y, Huang R, Bian J, Zheng C, Sun H, Chen Z, Sun N, An R, Min F, Zhao W, Zhuo Y, You J, Song Y, Yu Z, Liu Z, Yang K, Gao H, Dai H *et al* (2007) High-throughput synergy screening identifies microbial metabolites as combination agents for the treatment of fungal infections. *Proc Natl Acad Sci USA* **104:** 4606–4611

Zimmermann GR, Lehar J, Keith CT (2007) Multi-target therapeutics: when the whole is greater than the sum of the parts. *Drug Discov Today* **12:** 34–42